ORIGINAL ARTICLE

Contributions to
Plasma Physics

Insights into type-I edge localized modes and edge localized mode control from JOREK non-linear magneto-hydrodynamic simulations

M. Hoelzl[1] | **G.T.A. Huijsmans[2,3]** | **F. Orain[1]** | **F.J. Artola[4]** | **S. Pamela[5]** | **M. Becoulet[2]** |

D. van Vugt[3] | **F. Liu[2,6]** | **S. Futatani[7]** | **A. Lessig[1]** | **E. Wolfrum[1]** | **F. Mink[1]** | **E. Trier[1]** |

M. Dunne[1] | **E. Viezzer[1]** | **T. Eich[1]** | **B. Vanovac[8]** | **L. Frassinetti[9]** | **S. Guenter[1]** |

K. Lackner[1] | **I. Krebs[10]** | **ASDEX Upgrade Team[1]** | **EUROfusion MST1 Team****

[1]Max-Planck-Institute for Plasma Physics, Garching b. M., Germany
[2]CEA, IRFM, Saint-Paul-Lez-Durance, France
[3]Eindhoven University of Technology, Eindhoven, The Netherlands
[4]CNRS, Aix-Marseille University, Marseille Cedex 20, France
[5]CCFE, Culham Science Centre, Abingdon, UK
[6]Laboratoire J.A. Dieudonné UMR n∘ 7351 CNRS UNS, Université Côte d'Azur, Nice Cedex 02, France
[7]Barcelona Supercomputing Center, Barcelona, Spain
[8]DIFFER, Dutch Institute for Fundamental Energy Research, Eindhoven, The Netherlands
[9]Division of Fusion Plasma Physics, KTH Royal Institute of Technology, Stockholm, Sweden
[10]Princeton Plasma Physics Laboratory, Princeton, New Jersey, USA

*Correspondence
M. Hoelzl, Max-Planck-Institute for Plasma Physics, Boltzmannstr. 2, 85748 Garching b. M., Germany.
Email: matthias.hoelzl@ipp.mpg.de

Edge localized modes (ELMs) are repetitive instabilities driven by the large pressure gradients and current densities in the edge of H-mode plasmas. Type-I ELMs lead to a fast collapse of the H-mode pedestal within several hundred microseconds to a few milliseconds. Localized transient heat fluxes to divertor targets are expected to exceed tolerable limits for ITER, requiring advanced insights into ELM physics and applicable mitigation methods. This paper describes how non-linear magneto-hydrodynamic (MHD) simulations can contribute to this effort. The JOREK code is introduced, which allows the study of large-scale plasma instabilities in tokamak X-point plasmas covering the main plasma, the scrape-off layer, and the divertor region with its finite element grid. We review key physics relevant for type-I ELMs and show to what extent JOREK simulations agree with experiments and help reveal the underlying mechanisms. Simulations and experimental findings are compared in many respects for type-I ELMs in ASDEX Upgrade. The role of plasma flows and non-linear mode coupling for the spatial and temporal structure of ELMs is emphasized, and the loss mechanisms are discussed. An overview of recent ELM-related research using JOREK is given, including ELM crashes, ELM-free regimes, ELM pacing by pellets and magnetic kicks, and mitigation or suppression by resonant magnetic perturbation coils (RMPs). Simulations of ELMs and ELM control methods agree in many respects with experimental observations from various tokamak experiments. On this basis, predictive simulations become more and more feasible. A brief outlook is given, showing the main priorities for further research in the field of ELM physics and further developments necessary.

KEYWORDS

ballooning mode, ELM control, ELMs, JOREK, MHD, mode coupling, stochastic field, tokamak

1 | INTRODUCTION

When the high-confinement mode (H-mode) was discovered in 1982 in the Axially Symmetric Divertor Experiment (ASDEX) divertor tokamak, the authors also reported about "short bursts [...] which lead to periodic density and temperature

---

reductions in the outer plasma zone."[1] For these bursts, the name "edge localized modes (ELMs)" was given[2] and different classes of ELMs were identified as summarized, e.g. in refs [3, 4] Type-I ELMs are the largest and most common edge instability in H-mode plasmas associated with losses of typically up to 10% of the total plasma thermal energy and particles on a time scale of several hundred microseconds to a few milliseconds. For the International Thermonucleaar Experimental Reactor (ITER), regression analysis predicts relative ELM sizes larger than in present machines and divertor heat fluxes exceeding the limits acceptable for a reasonably long material lifetime.[5] Consequently, research on natural ELM-free regimes such as the quiescent H mode (QH-Mode),[6,7] ELM pacing via pellet injection[8] or magnetic kicks,[9] and ELM mitigation suppression via resonant magnetic perturbation fields (RMPs),[10] has come into the focus aiming to reduce divertor heat loads.

Linear magneto-hydrodynamic (MHD) analysis of the plasma stability has identified ideal ballooning modes as the main instability responsible for type-I ELM crashes, e.g. refs [11, 12] However, only non-linear simulations allow the investigation of the underlying non-linear physics processes of ELMs and the relevant control methods. A comprehensive review of non-linear simulations of ELMs and their control by various codes can be found in ref. [13].

The non-linear MHD code JOREK is described in Section 2. Section 3 reviews the key physics relevant for ELM crashes, and shows to which extent simulations agree with experiments and how they promote a basic understanding of ELM physics. On the example of ASDEX Upgrade,[14] we demonstrate that quantitative agreement is obtained between simulations and experiments in many respects. At the same time, a brief overview is given of recent ELM-related simulations performed with JOREK. Recent advances demonstrate that simulations are undergoing a transition from a qualitative description of ELM physics and ongoing validation towards predictive capabilities. An overview of ELM control methods is given in Section 4: ELM-free regimes, ELM pacing via pellet injection and magnetic kicks, as well as mitigation and suppression by RMPs. For each control method, the principles are briefly explained, and an overview of the results from JOREK is given. Conclusions and an outlook are provided in Section 5.

2 | THE JOREK CODE

The non-linear MHD code JOREK[15] allows the investigation of large-scale instabilities in divertor tokamaks. It applies a C^1 continuous flux-surface-aligned 2D Bezier mesh[16] and a toroidal Fourier representation to discretize the plasma, the scrape-off layer (SOL), and the divertor. Ideal wall boundary conditions and sheath boundary conditions at geometrically simplified divertor targets apply. The initial fields produced by a built-in Grad–Shafranov solver are advanced in time fully implicitly allowing the use of time steps independent of the grid resolution. The sparse matrix system is solved with an iterative GMRES scheme pre-conditioned by solving matrix blocks corresponding to individual toroidal harmonics using the direct sparse matrix solver PaStiX[17] (which is the limiting factor in terms of memory consumption and parallel scalability). A hybrid OpenMP/MPI approach is used for parallelization, where typically one or a few MPI tasks are used per compute node. Collaborative code development is performed via a shared git repository with automatic tests, code reviewing, and a documentation Wiki.

Results presented in this paper are based on a reduced MHD physics model, including neo-classical and diamagnetic effects,[18] which fulfils the energy conservation properties.[19] Full MHD equations are available[20] and presently being extended by two-fluid effects, sheath boundary conditions, and stabilization methods. A free boundary extension for coils and resistive walls replacing ideal wall conditions is realized via a coupling[21] to STARWALL.[22] A pellet ablation model,[23] a full-orbit particle tracer including ionization, recombination, and background collisions,[24] a neutrals model,[25] and a relativistic electron guiding center particle tracer[26] are available. An impurity model[27] and a relativistic electron fluid model are presently being validated.

JOREK is broadly applied to large-scale plasma instabilities in tokamak plasmas. ELM-related activities are the subject of this paper. Disruption-related research includes (neo-classical) tearing modes[28] and their control,[29] thermal and current quench including massive gas injection[25,27] and shattered pellet injection,[30] vertical displacement events,[31] as well as runaway electrons.[26,32]

3 | TYPE-I ELMS

This section reviews the key physics of type-I ELMs. Results from the ASDEX Upgrade ELM simulations are shown and compared with key features of experiments, giving some insight into basic mechanisms. An overview of recent research on ELM physics with JOREK is given as well.

3.1 | Set-up for the ASDEX Upgrade ELM simulations

The simulations shown in the following are based on a typical ASDEX Upgrade H-mode equilibrium with an edge safety factor $q_{95} = 5.9$. The experimentally observed type-I ELM crashes take about 2 ms corresponding to the so-called long ELMs.[33–35] A pre-ELM equilibrium reconstruction (ASDEX Upgrade discharge #33616 at 7.2 s) performed by the CLISTE code[36] is used for initial conditions, which is already unstable such that the simulations only allow the investigation of the ELM crash itself but not the inter-ELM phase. The plasma resistivity is increased from the Spitzer value by a factor of eight for computational reasons. The parallel heat diffusivity is taken to be two orders of magnitude smaller than Spitzer–Härm predictions[37] to account for the heat flux limit.[38,39] Neo-classical and diamagnetic flows are taken into account. Toroidal harmonics $n = 0 \ldots 8$ are included in the main simulations. Additional tests have been done to verify that mode numbers beyond $n = 8$ are sub-dominant. Linearly we have tested mode numbers up to 24, showing that high mode numbers are sub-dominant due to the stabilizing effects of ExB and diamagnetic flows. As a non-linear test, we have restarted our simulations with $n = 0 \ldots 13$ instead of $n = 0 \ldots 8$ for about 0.2 ms during the ELM crash. The $n = 9 \ldots 13$ harmonics remain by about one order of magnitude smaller than the $n = 3$, 4 modes dominant in this phase. Running the whole simulation with more harmonics is possible with the present code but computationally expensive. We will make use of that for cases where this is really necessary. In parallel, numerical work on the solver is performed in order to reduce the computational effort for large toroidal resolutions.

3.2 | Inter-ELM phase

After an ELM crash, pedestal pressure gradients are moderate. Consequently, edge current densities are low, which are dominated by the bootstrap current.[40] Also the $E \times B$ rotation is strongly reduced since it is in the pedestal region described by neo-classical physics.[41] Because of the H-mode transport barrier, the density and temperature pedestals start to build up.[42] In the experiments, the maximum pressure gradient in many cases increases up to a certain value and remains there for several milliseconds before an ELM crash occurs.[43] The EPED model[44] predicts that, when a critical pressure gradient for kinetic ballooning modes is reached, these modes lead to a clamping of the pressure gradient. A correlation of this clamping with high-frequency modes has been confirmed experimentally,[45,46] although Laggner et al. could not confirm the ballooning character of the observed modes. Typically, while the maximum pressure gradient remains clamped, the pedestal grows further inwards until a large ELM crash appears. Often, precursor modes are observed before, which have a similar spatial structure as the ELM crash.[47,48] JOREK simulations so far did not concentrate strongly on the inter-ELM phase. Multiple ELM cycles have been obtained,[49,50] with artificially increased sources such that repetition frequencies are higher than for type-I ELMs. Refined simulations will investigate realistic type-I ELM cycles and give a deeper insight into inter-ELM phase and ELM onset.

3.3 | Linear growth of the instability

In the ASDEX Upgrade ELM simulations, the linear instability growing out of a small non-axisymmetric initial perturbation is dominated by the $n = 6$ toroidal harmonic (see Figure 1) with an eigenfunction localized to the outboard side of the plasma, as is typical for ballooning modes.* This is in line with the fact that the precursor modes observed prior to the ELM crash in these ASDEX Upgrade experiments are also localized to the outboard side of the plasma. The linear growth rate for the magnetic perturbation of $4 \pm 1 \times 10^4 \, \mathrm{s}^{-1}$ agrees well with the experimental value of $5 \pm 2 \times 10^4 \, \mathrm{s}^{-1}$ obtained by magnetic measurements; however, the higher resistivity in the simulations as well as uncertainties in the equilibrium reconstruction can affect this comparison.

Neo-classical and diamagnetic flows[51] are crucial for reproducing the key experimental observations. Without flows, far larger mode numbers become linearly dominant, which is in line with infinite-n ballooning predictions and previous ASDEX Upgrade simulations that had not accounted for flow effects.[21] As a result, simulations without background flows lead to a spectrum during the crash, which is very different from experimental observations. The ratio of energy lost to the inner and outer divertor targets is close to experimental observations only when flows are included (see Section 3.6). Finally, these flows are necessary to reproduce experimental mode rotation.[52]

3.4 | Quadratic mode coupling

Quadratic mode coupling sets in significantly before the instability has reached a large enough amplitude to affect the background profiles and begins to saturate (compare also ref. [53]). In the present case, for instance, the $n = 5$ and $n = 6$ harmonics are driving the $n = 1$ mode as seen in the left part of Figure 1, which is linearly stable. The right part of the figure shows, on a non-logarithmic scale, the further evolution of energies across the ELM crash.
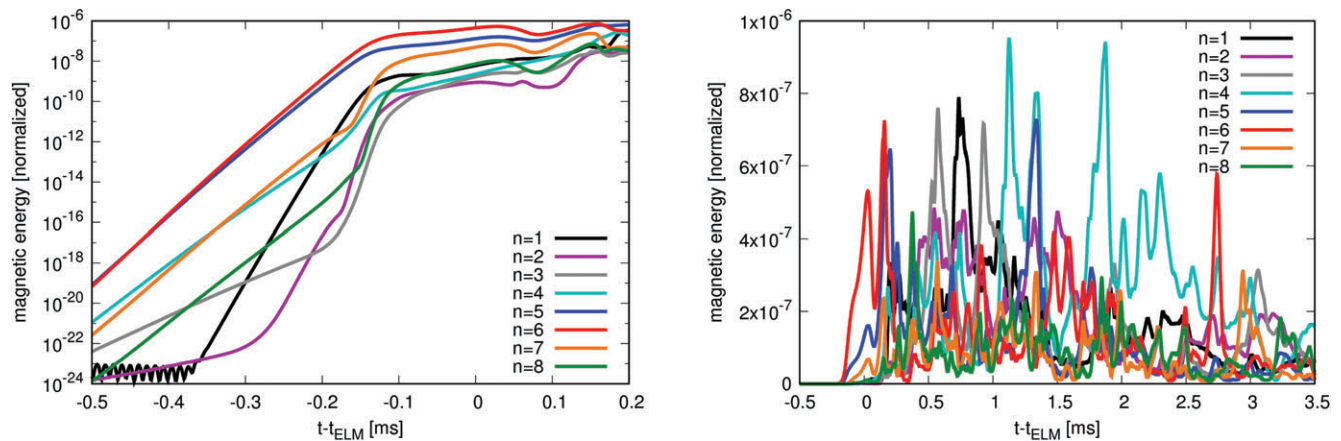
FIGURE 1 Evolution of magnetic energies for the individual harmonics versus time. *Left*: Logarithmic plot of the early edge localized mode (ELM) phase showing the drive of sub-dominant modes by linear mode coupling. *Right*: Non-logarithmic plot showing that the perturbations are strongest at $t - t_{ELM} = 0 \ldots 2$ ms where divertor heat fluxes are high, while some activity remains after the crash and decays away relatively slowly

There are various indications from experiments on the importance of quadratic mode coupling during ELM crashes. Strong low-n components were reported, for instance, in the TCV tokamak,[54] which cannot be explained by linear stability analysis. Also magnetic structures observed during ELMs which are strongly localized to certain magnetic field lines and which consist of a large number of coherent modes[21,55] are indicative of mode coupling. Very recently, direct evidence of three-wave coupling during an ELM cycle was reported for ASDEX Upgrade in the discharge discussed here.[56]

Refined evaluation methods for the magnetic measurements at ASDEX Upgrade[57] allows the extraction of the toroidal spectrum during an ELM cycle, revealing dominant $n = 2 \ldots 5$ components[47] for the present discharge, corresponding to a clear shift from the linear stability analysis in which $n = 5, 6$ are dominating.† In the simulation, $n = 4$ is dominating during the ELM crash ($t - t_{ELM} = 0 \ldots 2$ ms),‡ $n = 1 \ldots 6$ have significant amplitudes, and $n \geq 7$ are lower by at least a factor two in average energies. The $n = 1$ mode is important for the development of the non-linear spectrum during the ELM crash as demonstrated by the fact that identical simulations restricted to the $n = 0, 2, 4, 6, 8$ or $n = 0, 3, 6, 9$ harmonics lead to an ELM crash almost entirely dominated by $n = 6$.

In summary, the growth rate and the toroidal mode spectrum during the ELM crash are reproduced well in simulations if neo-classical and diamagnetic effects are included and the coupling to the $n = 1$ harmonic is taken into account. Recent experimental studies for ASDEX Upgrade suggest a strong dependence of the dominant toroidal mode number on q_{95}[58] (or the plasma current), opening up promising opportunities for further comparisons.

3.5 | Loss mechanisms

The ballooning modes leading to the ELM crash are associated with a strong kinetic as well as a magnetic perturbation of the plasma, leading to two different loss mechanisms.

3.5.1 | Convective losses

The kinetic perturbation leads to the formation of ballooning fingers by an interchange-like $E \times B$ inward/outward motion of low/high-pressure plasma at the very edge. The high-pressure fingers in the SOL are partly sheared off by plasma flows induced during the crash by Maxwell stress, leading to the formation of filaments elongated along the magnetic field lines as shown in Figure 2. Several such bursts are observed, which is in line with experimental observations for long type-I ELMs.[34] The high-pressure structures expelled into the SOL quickly lose energy towards the divertor by parallel heat conduction, whereas the heat flux onto the main walls is typically low since the time scale for parallel conduction to the divertors is usually much shorter than the time scale for the filament convection to the wall. This is also the case in the present simulation, where the filaments have lost most of their energy before they come close to the wall.

3.5.2 | Conductive losses

The magnetic perturbations produced by the instabilities lead to the formation of islands. At larger amplitudes where these islands begin to overlap, flux surfaces are destroyed and a stochastic field region is formed.[60] As seen in Figure 3, the edge of the plasma becomes fully stochastic. The magnetic field lines in this region are directly connected to the divertor targets as the
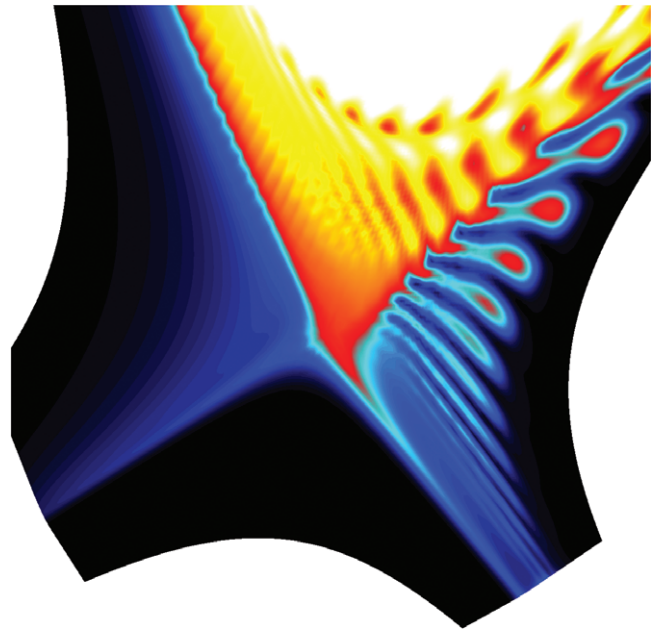
FIGURE 2 Pressure distribution around the X-point during an edge localized mode (ELM) simulation. The formation of filaments can be observed, which quickly lose their pressure along magnetic field lines outside the separatrix. This simulation (taken from ref. [59]) does not include background flows. When background flows are taken into account, ballooning fingers and filament formation are still observed in simulations, but the separation of the filaments from the main plasma becomes less pronounced
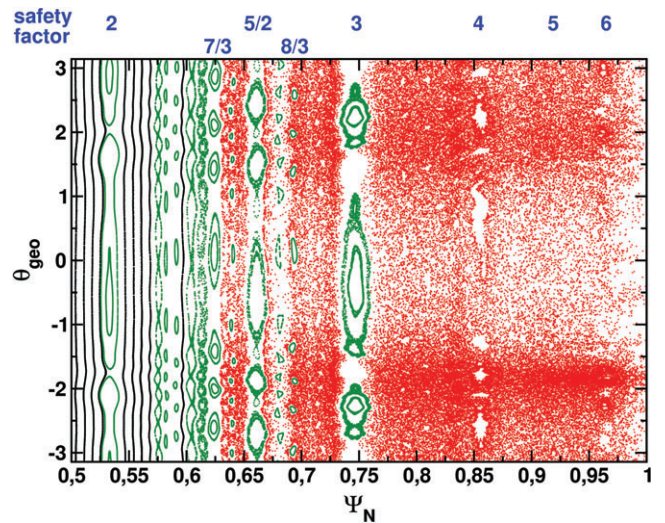

FIGURE 3 Poincaré plot of the magnetic structure at $t - t_{\text{ELM}} = 1.21$ ms. Stochastic regions are shown in red, islands in green, and normal closed flux surfaces in black. In the region outside the $q = 3$ surface, KAM surfaces have broken down such that a single stochastic region is formed. The stochastic regions inside $q = 3$ are separated by intact KAM surfaces as also seen in the connection length plot (Figure 4)

connection length plot of Figure 4 shows. However, from the $q = 3$ surface inwards, some of the Kolmogorov-Arnold-Moser (KAM) surfaces remain intact, forming "magnetic barriers"[62–65]. As a result, although stochastization is observed inside the $q = 3$ surface, the connection length to the divertor targets remains infinite for this region. Figure 4 also shows experimental data for the propagation of the cold front produced by the ELM crash, which qualitatively agrees well with the evolution of the stochastic layer.

The region affected by convection due to the formation of ballooning fingers typically contains a larger fraction of the plasma particles than of the plasma thermal energy due to the very different density and temperature profiles. In the considered ASDEX Upgrade equilibrium, the region $\Psi_N = 0.95\ldots1$ contains about 6.6% of the particles and only 2.0% of the thermal energy. These numbers represent the upper limits for the possible convective losses showing that convective losses predominantly lead to particle losses. Conductive losses along the stochastic magnetic field lines mostly affect the electron temperature due to the large parallel electron heat conductivity.

In the present simulation, about 7% of the particles and 3% of the thermal energy are lost during the ELM crash, while the experiment sees values of $8 \pm 1\%$ of particle losses and $6 \pm 1\%$ of energy losses. Thus, the particle losses agree well, while the energy losses are underestimated in the simulation. This indicates that our choice of the parallel heat diffusion coefficient (reduced by two orders of magnitude compared to the Spitzer values in order to account for the heat flux limit) is not appropriate. A proper treatment of the heat flux limit will be implemented for future simulations. The ELM duration defined by the time during which significant losses and divertor heat fluxes are observed is about 2 ms both in the experiment and simulations, corresponding to the so-called long ELMs.[33,34]
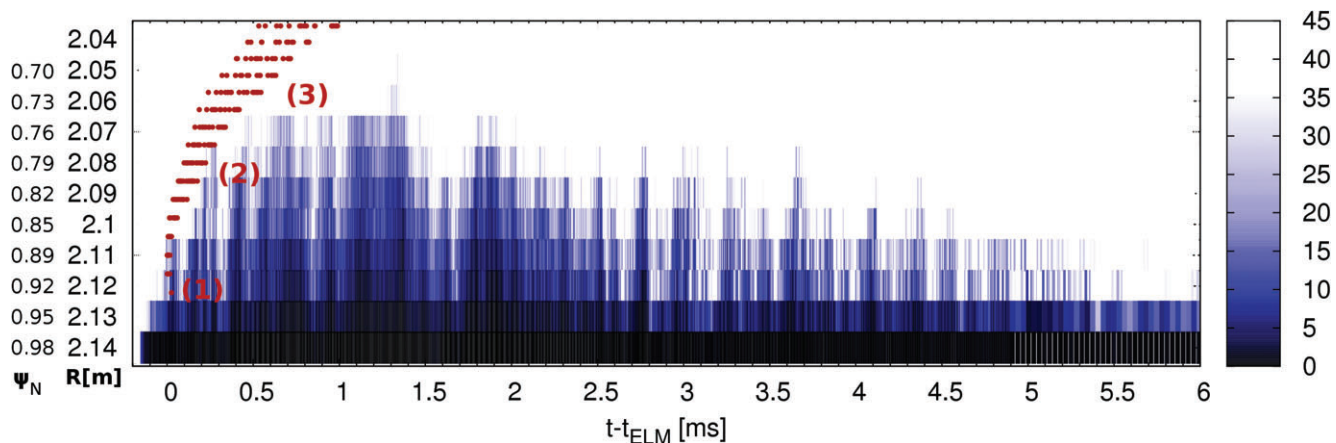
FIGURE 4   Connection length (in km) at various radial locations from the mid-plane to the divertor targets along magnetic field lines plotted over time (white: no connection to the divertor). Stochasticity appears with a very fast first burst at $t - t_{ELM} = 0$ ms and successively grows further inwards within $\approx 300\ \mu$s. Both in the time scales and the radial region, the stochastic layer formation agrees well with the cold front propagation measured in experiments (red dots, see ref. [61] for a detailed analysis) obtained for similar plasma configurations (same plasma current). In the very edge, almost instantaneous propagation probably due to the first stochastic burst and convective losses (1), then propagation on a fast time scale following roughly the growth of the edge stochastic layer connected to the divertor targets (2), and further inwards slower propagation supposedly dominated by islands and local stochastic field regions (3) are seen. After the main edge localized mode (ELM) crash ($t - t_{ELM} > 2$ ms), the stochastic region disappears slowly

3.6 | Divertor heat loads

In ASDEX Upgrade and other devices,[66,67] the total heat fluxes towards the inner and outer divertor are comparable in normal magnetic field orientation. In the present ASDEX Upgrade simulations, about 40% of the energy is transported towards the inner divertor and 60% towards the outer divertor, comparable to the experimental observations. In simulations without neo-classical and diamagnetic flows, a much stronger heat flux towards the outer divertor is observed.[68] Since the experiment observes a pronounced heat flux towards the outer divertor in reversed field operation[66,67] additional comparisons will be performed to verify whether this trend is reproduced.

The peak heat fluences in JET ELM simulations were compared for a large number of equilibria[69,70] to the experimentally observed scaling. [71] Simulations without background flows show excellent agreement regarding energy losses and peak heat fluences; however, they do not reproduce the distribution of heat between the inner and outer divertor legs of the experiments. Simulations including background flows reproduce well the distribution between inner and outer divertor legs but underestimate ELM energy losses and peak heat fluences. Thus, in spite of the very encouraging agreement in this respect, the remaining inconsistencies are under investigation.

3.7 | Decay of the MHD activity

The drop of edge pressure gradient and current density in the pedestal region during the ELM crash acts to stabilize the linear instability. On the other hand, the stabilizing $E \times B$ and diamagnetic flows are reduced as well, since they follow the pressure gradient evolution. Also, the ELM crash is associated with strongly localized structures such that even when the flux-surface-averaged pressure profiles are flattened considerably, large local gradients may be present. Similar to the recently observed ballooning modes localized to certain field lines with applied RMP fields,[72] this can give rise to local instabilities. As a result, the instability does not decay away as fast as would be expected from the simplified linear pictures. The mechanism for the formation of short and long ELMs, often even in the same discharge, is under investigation in experiments (see e.g. refs [34, 73]) and will also be studied in future simulations. The interplay of stabilizing and destabilizing effects is also crucial for the formation of cyclic ELM crashes. Based on first demonstrations of multiple ELM cycle simulations[49,50] with repetition frequencies significantly higher than for type-I ELMs, we will continue our efforts to reproduce full type-I ELM cycles.

3.8 | Tungsten transport

In order to obtain good performance of ITER, the impurity concentration in the plasma needs to be kept below certain thresholds. Tungsten is a particularly important impurity since it is used as divertor material and is not completely ionized even at temperatures of several kiloelectronvolts, leading to strong radiative losses. ELMs can control the tungsten concentration in the plasma by expelling tungsten particles. The full orbit particle tracer of JOREK,[24,74] which accounts for the evolution of ionization states, allows the study of this phenomenon.

Based on ASDEX Upgrade ELM simulations discussed in the previous sections, tungsten transport is investigated.[§] Several million test particles are initialized, covering the whole relevant area ranging from the outer core plasma to the SOL. During the ELM crash, a strong radial mixing is observed. The radial motion of the particles is caused by the perturbation of the electric field during the crash. Within 1 ms of the ELM crash, about 10% of the particles from the pedestal region ($\Psi_N = 0.95\ldots1$) are lost across the separatrix, while about 15% of the particles from the SOL ($\Psi_N = 1\ldots1.05$) are transferred into the plasma. Thus, if the tungsten particle density inside the separatrix is much larger than in the SOL before the ELM crash,[75] a significant net exhaust of tungsten particles is observed. A detailed analysis will be presented in a separate paper.

4 | ELM CONTROL

The strong localized heat loads onto divertor targets expected in ITER have given rise to research on various approaches for ELM control. At the same time, a sufficient ELM frequency (or substitution by different mechanisms) is important to keep the impurity concentration in the plasma at a tolerable level. This section gives a brief overview of the most relevant approaches for ELM control. The basic principles are explained referring to related simulations.

4.1.1 | Quiescent H-mode

Natural ELM-free regimes, such as the quiescent H-mode (QH mode)[6,7], have been found in various tokamak experiments and are an important subject of present studies. The QH mode is characterized by a pedestal comparable to that of H-mode plasmas, the absence of ELM crashes, and a saturated rotating mode in the pedestal region causing a characteristic perturbation of density and temperature (edge harmonic oscillation, EHO). The QH mode seems to be obtained best with strong plasma shaping, large edge current densities (i.e. low collisionalities), strong edge flow shears, and in reversed field operation. Key aspects of the QH mode, such as the saturated modes in the pedestal region with low toroidal mode numbers and the resulting EHO, have been reproduced sucessfully in JOREK simulations,[76,77] identifying the EHO as a saturated kink-peeling mode. These modes induce enhanced particle transport across the pedestal region, which is beneficial for limiting the impurity accumulation in the plasma. Non-linear mode coupling leads to the toroidal localization of the EHO. The mechanisms determining whether a certain plasma configuration enters an ELMing H-mode or QH mode are under investigation.

4.1.2 | Pellet ELM triggering

The injection of pellets to trigger ELMs more frequently than they would occur naturally[8] has proven successful in many experiments and allows the reduction of ELM energy losses.[78] Whether the peak heat fluxes can also be mitigated with this method is not definitely answered. The mechanism of pellet ELM triggering[23,79–81] has been identified by JOREK simulations of pellet injection. When the pellet ablates adiabatically, the pressure in the pellet cloud remains unchanged while the electron density is strongly increased and the temperature is strongly decreased. Because of the fast heat transport along magnetic field lines, the pellet cloud is re-heated faster than the density decreases by parallel convection. Thus, a strong 3D perturbation of the pressure forms, driving the plasma locally beyond the ballooning stability threshold such that an ELM crash sets in. Simulations for DIII-D have demonstrated a clear threshold in the pellet size for destabilizing ELMs, which agrees reasonably well with the experimental observations.[23] Validation against other devices as well as predictive simulations for ITER are going on. Additionally, simulations are presently refined by the inclusion of background flows.

4.1.3 | Vertical kick ELM triggering

The destabilization of ELMs by magnetic kicks was demonstrated in several tokamak devices.[9,78] Although destabilization due to an increase of the edge current density was suspected, the exact mechanisms remained unclear. Recent simulations with the free-boundary JOREK-STARWALL[21] for a realistic ITER 7.5MA/2.65T plasma have now shown that ELMs are indeed destabilized by an increase of the edge current density.[82] The mechanisms changing the current density have been revealed to be strongly related to plasma compression, allowing the optimization of the coil current time traces for kicks. In line with experimental observations, the destabilization always appears at the same vertical axis position independent of the kick velocity for a given equilibrium. Additionally, a plasma that is already peeling-ballooning unstable can be driven back into the stable regime by a kick in the opposite direction, explaining that with the sinusoidal kicks performed in experiments ELMs always occur in a particular phase during which the plasma is compressed by the kick. After additional validation against existing experiments in the JET tokamak, how the peak heat fluxes of the triggered ELMs compare with natural ELMs[§] will be investigated.

4.1.4 | Mitigation or suppression by RMP fields

Mitigation and suppression of ELMs by the application of RMPs has been observed in various experiments.[10,83] Early JOREK simulations of the penetration of RMP fields into the plasma[84] have been refined by the inclusion of two-fluid effects,[85,86] reproducing well the 3D displacement of the flux surfaces observed in the experiments. The mitigation and suppression of ELMs is presently thought to be caused by either edge stochastization or the presence of a magnetic island at the pedestal top, reducing the pressure gradient in the pedestal below the peeling-ballooning threshold. However, JOREK simulations[85,87] indicate that non-linear mode coupling can play an important role as well. In ref. [87], it is shown for the ASDEX Upgrade geometry that RMP fields can hinder ballooning modes from growing exponentially. This is observed only in the so-called resonant configuration of RMP coil currents, consistent with ELM suppression in ASDEX Upgrade experiments. The exact mechanisms are under investigation.

5 | CONCLUSIONS

An overview of the JOREK code and its recent applications to ELM physics was given. Many key features of type-I ELMs and of ELM control methods from the experiments were reproduced very well in the simulations so that predictive simulations become more and more feasible.

A type-I ELM crash in ASDEX Upgrade was compared in detail to the experimental observations. The linear instability has ballooning character, as is also seen for modes just before the ELM onset in the experiment, and the linear growth rates agree well. Because of quadratic mode coupling, the $n = 4$ mode dominates during the ELM crash, which is comparable to the dominant $n = 3$ mode in the experiment (the dependency of the dominant mode number on various plasma parameters is under investigation experimentally and in simulations). Also, neo-classical and diamagnetic flows are crucial for obtaining a mode spectrum comparable to that in the experiment. Recent experimental observations directly prove the mode coupling during an ELM cycle. The ELM crash takes about 2 ms both in experiment and simulations ("long ELM"). The convective losses due to the formation of ballooning fingers and the conductive losses due to the formation of a stochastic layer in the plasma edge were discussed in detail. The evolution of the stochastic layer agrees well with the experimentally observed propagation of the ELM cold front. Total particle losses during the ELM agree very well between experiment and simulations, while losses of the thermal energy are underestimated in the simulations. Most likely, this is due to an underestimation of conductive losses by the applied parallel heat diffusivity. The ELM heat load is almost evenly distributed between the inner (40%) and the outer (60%) divertor target in line with experimental observations for normal field operation. Without the inclusion of neo-classical and diamagnetic flows, almost the entire heat load goes to the outer divertor target. Tungsten transport by the ELM crash is under investigation and shows already good qualitative agreement with the experiment; quantitative comparisons are going on. Published results for JET show good agreement of peak heat fluences with experimental scaling. However, when background flows are included, heat fluences are underestimated, which needs further investigations.

Regarding ELM control, a brief overview of JOREK activities in the fields of QH mode, pellet ELM triggering, magnetic kick ELM triggering, and ELM mitigation/suppression by RMP fields was given.

Future activities will concentrate on improving the models to further improve the agreement with the experiment. This will include, for instance, pushing simulations to fully realistic resistivity values, improving the SOL model. Additional validation will be done based on observations from various devices both for ELM crashes as well as for the control methods, which are under investigation. Based on this, predictions for ITER will be possible more and more accurately. Obtaining fully realistic type-I ELM cycles is an important goal, allowing the study of also the inter-ELM phase and the ELM onset in detail. Understanding the differences between short and long ELMs and small ELM regimes will be important research topics as well.

NOTES

∗ The $n = 5$ growth rate is only slightly lower than the $n = 6$ growth rate.
† Note, that the method applied cannot resolve $n = 1$ due to the large wavelength and short time scales involved such that the $n = 1$ amplitude remains unknown in the experiment.

‡ Note that t_{ELM} is defined as the time when the heat flux in the outer divertor starts to rise significantly in order to be comparable with the experiment. The ELM crash is completed after about 2 ms, since losses and divertor heat fluxes drop significantly at that point.

§ Background collisions have not been accounted since the collision time of tungsten ions with the background plasma assuming a 1% beryllium concentration is longer than the time scale of MHD fluctuations.

ORCID

M. Hoelzl http://orcid.org/0000-0001-7921-9176

REFERENCES

[1] F. Wagner, G. Becker, K. Behringer, D. Campbell, A. Eberhagen, W. Engelhardt, G. Fussmann, O. Gehre, J. Gernhardt, G. v. Gierke, G. Haas, M. Huang, F. Karger, M. Keilhacker, O. Klüber, M. Kornherr, K. Lackner, G. Lisitano, G. G. Lister, H. M. Mayer, D. Meisel, E. R. Müller, H. Murmann, H. Niedermeyer, W. Poschenrieder, H. Rapp, H. Röhr, F. Schneider, G. Siller, E. Speth, A. Stäbler, K. H. Steuer, G. Venus, O. Vollmer, Z. Yü, *Phys. Rev. Lett.* **1982**, *49*, 1408.

[2] M. Keilhacker, G. Becker, K. Bernhardi, A. Eberhagen, M. ElShaer, G. FuBmann, O. Gehre, J. Gernhardt, G. v. Gierke, E. Glock, G. Haas, F. Karger, S. Kissel, O. Kluber, K. Kornherr, K. Lackner, G. Lisitano, G. G. Lister, J. Massig, H. M. Mayer, K. McCormick, D. Meisel, E. Meservey, E. R. Muller, H. Murmann, H. Niedermeyer, W. Poschenrieder, H. Rapp, B. Richter, H. Rohr, F. Ryter, F. Schneider, S. Siller, P. Smeulders, F. Soldner, E. Speth, A. Stabler, K. Steinmetz, K.-H. Steuer, Z. Szymanski, G. Venus, O. Vollmer, F. Wagner, *Plasma Phys. Controll. Fusion* **1984**, *26*(1A), 49.

[3] E. J. Doyle, R. J. Groebner, K. H. Burrell, P. Gohil, T. Lehecka, N. C. L. Jr, H. Matsumoto, T. H. Osborne, W. A. Peebles, R. Philipona, *Phys. Fluids B Plasma Phys.* **1991**, *3*, 2300. https://doi.org/10.1063/1.859597.

[4] H. Zohm, *Plasma Phys. Controll. Fusion* **1996**, *38*(2), 105.

[5] A. Loarte, G. Saibene, R. Sartori, D. Campbell, M. Becoulet, L. Horton, T. Eich, A. Herrmann, G. Matthews, N. Asakura, A. Chankin, A. Leonard, G. Porter, G. Federici, G. Janeschitz, M. Shimada, M. Sugihara, *Plasma Phys. Controll. Fusion* **2003**, *45*, 1549.

[6] K. H. Burrell, M. E. Austin, D. P. Brennan, J. C. DeBoo, E. J. Doyle, P. Gohil, C. M. Greenfield, R. J. Groebner, L. L. Lao, T. C. Luce, M. A. Makowski, G. R. McKee, R. A. Moyer, T. H. Osborne, M. Porkolab, T. L. Rhodes, J. C. Rost, M. J. Schaffer, B. W. Stallard, E. J. Strait, M. R. Wade, G. Wang, J. G. Watkins, W. P. West, L. Zeng, *Plasma Phys. Controll. Fusion* **2002**, *44*(5A), A253.

[7] C. M. Greenfield, K. H. Burrell, J. C. DeBoo, E. J. Doyle, B. W. Stallard, E. J. Synakowski, C. Fenzi, P. Gohil, R. J. Groebner, L. L. Lao, M. A. Makowski, G. R. McKee, R. A. Moyer, C. L. Rettig, T. L. Rhodes, R. I. Pinsker, G. M. Staebler, W. P. West, the DIII-D Team, *Phys. Rev. Lett.* **2001** May, *86*, 4544.

[8] P. T. Lang, H. Zohm, K. Buchl, J. C. Fuchs, O. Gehre, O. Gruber, V. Mertens, H. W. Muller, J. Neuhauser, *Nucl. Fusion* **1996**, *36*, 1531.

[9] A. W. Degeling, Y. R. Martin, J. B. Lister, L. Villard, V. N. Dokouka, V. E. Lukash, R. R. Khayrutdinov, *Plasma Phys. Controll. Fusion* **2003**, *45*, 1637.

[10] T. E. Evans, M. E. Fenstermacher, R. A. Moyer, T. H. Osborne, J. G. Watkins, P. Gohil, I. Joseph, M. J. Schaffer, L. R. Baylor, M. BÃlcoulet, J. A. Boedo, K. H. Burrell, J. S. de Grassie, K. H. Finken, T. Jernigan, M. W. Jakubowski, C. J. Lasnier, M. Lehnen, A. W. Leonard, J. Lonnroth, E. Nardon, V. Parail, O. Schmitz, B. Unterberg, W. P. West, *Nucl. Fusion* **2008**, *48*, 024002.

[11] P. Gohil, M. Ali Mahdavi, L. Lao, K. H. Burrell, M. S. Chu, J. C. DeBoo, C. L. Hsieh, N. Ohyabu, R. T. Snider, R. D. Stambaugh, R. E. Stockdale, *Phys. Rev. Lett.* **1988** October, *61*, 1603.

[12] P. B. Snyder, H. R. Wilson, J. R. Ferron, L. L. Lao, A. W. Leonard, D. Mossessian, M. Murakami, T. H. Osborne, A. D. Turnbull, X. Q. Xu, *Nucl. Fusion* **2004**, *44*(2), 320.

[13] G. T. A. Huijsmans, C. S. Chang, N. Ferraro, L. Sugiyama, F. Waelbroeck, X. Q. Xu, A. Loarte, S. Futatani, *Phys. Plasmas* **2015**, *22*, 021805. https://doi.org/10.1063/1.4905231.

[14] U. Stroth, J. Adamek, L. Aho-Mantila, S. Äkäslompolo, C. Amdor, C. Angioni, M. Balden, S. Bardin, L. Barrera Orte, K. Behler, E. Belonohy, A. Bergmann, M. Bernert, R. Bilato, G. Birkenmeier, V. Bobkov, J. Boom, C. Bottereau, A. Bottino, F. Braun, S. Brezinsek, T. Brochard, M. Brüdgam, A. Buhler, A. Burckhart, F. J. Casson, A. Chankin, I. Chapman, F. Clairet, I. G. J. Classen, J. W. Coenen, G. D. Conway, D. P. Coster, D. Curran, F. da Silva, P. de Marné, R. D'Inca, D. Douai, R. Drube, M. Dunne, R. Dux, T. Eich, H. Eixenberger, N. Endstrasser, K. Engelhardt, B. Esposito, E. Fable, R. Fischer, H. Fünfgelder, J. C. Fuchs, K. Gál, M. García Muñoz, B. Geiger, L. Giannone, T. Görler, S. da Graca, H. Greuner, O. Gruber, A. Gude, L. Guimarais, S. Günter, G. Haas, A. H. Hakola, D. Hangan, T. Happel, T. Härtl, T. Hauff, B. Heinemann, A. Herrmann, J. Hobirk, H. Höhnle, M. Hölzl, C. Hopf, A. Houben, V. Igochine, C. Ionita, A. Janzer, F. Jenko, M. Kantor, C. P. Käsemann, A. Kallenbach, S. Kálvin, M. Kantor, A. Kappatou, O. Kardaun, W. Kasparek, M. Kaufmann, A. Kirk, H. J. Klingshirn, M. Kocan, G. Kocsis, C. Konz, R. Koslowski, K. Krieger, M. Kubic, T. Kurki-Suonio, B. Kurzan, K. Lackner, P. T. Lang, P. Lauber, M. Laux, A. Lazaros, F. Leipold, F. Leuterer, S. Lindig, S. Lisgo, A. Lohs, T. Lunt, H. Maier, T. Makkonen, K. Mank, M. E. Manso, M. Maraschek, M. Mayer, P. J. McCarthy, R. McDermott, F. Mehlmann, H. Meister, L. Menchero, F. Meo, P. Merkel, R. Merkel, V. Mertens, F. Merz, A. Mlynek, F. Monaco, S. Müller, H. W. Müller, M. Münich, G. Neu, R. Neu, D. Neuwirth, M. Nocente, B. Nold, J. M. Noterdaeme, G. Pautasso, G. Pereverzev, B. Plöckl, Y. Podoba, F. Pompon, E. Poli, K. Polozhiy, S. Potzel, M. J. Püschel, T. Pütterich, S. K. Rathgeber, G. Raupp, M. Reich, F. Reimold, T. Ribeiro, R. Riedl, V. Rohde, G. . Rooij, J. Roth, M. Rott, F. Ryter, M. Salewski, J. Santos, P. Sauter, A. Scarabosio, G. Schall, K. Schmid, P. A. Schneider, W. Schneider, R. Schrittwieser, M. Schubert, J. Schweinzer, B. Scott, M. Sempf, M. Sertoli, M. Siccinio, B. Sieglin, A. Sigalov, A. Silva, F. Sommer, A. Stäbler, J. Stober, B. Streibl, E. Strumberger, K. Sugiyama, W. Suttrop, T. Tala, G. Tardini, M. Teschke, C. Tichmann, D. Told, W. Treutterer, M. Tsalas, M. A. van Zeeland, P. Varela, G. Veres, J. Vicente, N. Vianello, T. Vierle, E. Viezzer, B. Viola, C. Vorpahl, M. Wachowski, D. Wagner, T. Wauters, A. Weller, R. Wenninger, B. Wieland, M. Willensdorfer, M. Wischmeier, E. Wolfrum, E. Würsching, Q. Yu, I. Zammuto, D. Zasche, T. Zehetbauer, Y. Zhang, M. Zilker, H. Zohm, *Nucl. Fusion* **2013**, *53*, 104003.

[15] G. T. A. Huysmans, O. Czarny, *Nucl. Fusion* **2007**, *47*(7), 659.

[16] O. Czarny, G. Huysmans, *J. Comput. Phys.* **2008**, *227*, 7423.

[17] P. Hénon, P. Ramet, J. Roman, *Parallel Comput.* **2002**, *28*(2), 301.

[18] F. Orain, M. Bécoulet, G. Dif-Pradalier, G. Huijsmans, S. Pamela, E. Nardon, C. Passeron, G. Latu, V. Grandgirard, A. Fil, A. Ratnani, I. Chapman, A. Kirk, A. Thornton, M. Hoelzl, P. Cahyna, *Phys. Plasmas* **2013**, *20*, 102510. https://doi.org/10.1063/1.4824820.

[19] E. Franck, M. Hoelzl, A. Lessig, E. Sonnendrücker, *ESAIM: M2AN* **2015**, *49*, 1331.

[20] J. W. Haverkort, H. J. de Blank, G. T. A. Huysmans, J. Pratt, B. Koren, *J. Comput. Phys.* **2016**, *316*, 281.

[21] M. Hoelzl, S. Guenter, R. P. Wenninger, W.-C. Mueller, G. T. A. Huysmans, K. Lackner, I. Krebs, *Phys. Plasmas* **2012**, *19*, 082505. https://doi.org/10.1063/1.4742994.

[22] P. Merkel, E. Strumberger, *arixv* **2015**, 1508.04911.

[23] S. Futatani, G. Huijsmans, A. Loarte, L. R. Baylor, N. Commaux, T. C. Jernigan, M. E. Fenstermacher, C. Lasnier, T. H. Osborne, B. PegouriÃl, *Nucl. Fusion* **2014**, *54*, 073008.

[24] D. C. van Vugt, G. T. A. Huijsmans, M. Hoelzl, L. P. J. Kamp, N. J. Lopes Cardoso, A. Loarte, in *44th European Physical Society Conference on Plasma Physics (EPS)*, Belfast, Northern Ireland.

[25] A. Fil, E. Nardon, M. Hoelzl, G. T. A. Huijsmans, F. Orain, M. Becoulet, P. Beyer, G. Dif-Pradalier, R. Guirlet, H. R. Koslowski, M. Lehnen, J. Morales, S. Pamela, C. Passeron, C. Reux, F. Saint-Laurent, *Phys. Plasmas* **2015**, *22*, 062509. https://doi.org/10.1063/1.4922846.

[26] C. Sommariva, E. Nardon, P. Beyer, M. Hoelzl, G. T. A. Huysmans, D. van Vugt, JET Contributors, *Nucl. Fusion* **2018**, *58*, 016043.

[27] E. Nardon, A. Fil, M. Hoelzl, G. Huijsmans, JET Contributors, *Plasma Phys. Controll. Fusion* **2017**, *59*, 014006.

[28] D. Meshcheriakov, V. Igochine, S. Fietz, M. Hoelzl, F. Orain, S. Günter, H. Zohm, in *44th European Physical Society Conference on Plasma Physics (EPS)*, Belfast, Northern Ireland.

[29] J. Pratt, G. T. A. Huijsmans, E. Westerhof, *Phys. Plasmas* **2016**, *23*, 102507. https://doi.org/10.1063/1.4964785.

[30] D. Hu, E. Nardon, G. T. A. Huijsmans, M. Lehnen, in *44th European Physical Society Conference on Plasma Physics (EPS)*, Belfast, Northern Ireland, pp. P2.142.

[31] M. Hoelzl, G. T. A. Huijsmans, P. Merkel, C. Atanasiu, K. Lackner, E. Nardon, K. Aleynikova, F. Liu, E. Strumberger, R. McAdams, I. Chapman, A. Fil, *J. Phys. Conf. Ser.* **2014**, *561*, 012011.

[32] V. Bandaru, M. Hoelzl, G. Papp, P. Aleynikov, G. Huijsmans, Implementation of a fluid model for the non-linear interaction between runaway electrons and background plasma. 17th European Fusion Theory Conference, Athens, Greece, O.5 (10/2017).

[33] L. Frassinetti, D. Dodt, M. N. A. Beurskens, A. Sirinelli, J. E. Boom, T. Eich, J. Flanagan, C. Giroud, M. S. Jachmich, M. Kempenaars, P. Lomas, G. Maddison, C. Maggi, R. Neu, I. Nunes, C. P. von Thun, B. Sieglin, M. Stamp, JET-EFDA Contributors, *Nucl. Fusion* **2015**, *55*, 023007.

[34] L. Frassinetti, M. G. Dunne, M. Beurskens, E. Wolfrum, A. Bogomolov, D. Carralero, M. Cavedon, R. Fischer, F. M. Laggner, R. M. McDermott, H. Meyer, G. Tardini, E. Viezzer, the EUROfusion MST1 Team, the ASDEX-Upgrade Team, *Nucl. Fusion* **2017**, *57*, 022004.

[35] B. Sieglin, T. Eich, A. Scarabosio, G. Arnoux, I. Balboa, S. Devaux, A. Herrmann, F. Hoppe, M. Hoelzl, A. Kallenbach, P. Lang, G. F. Matthews, S. Marsen, S. Pamela, M. Rack, R. Wenninger, the ASDEX Upgrade Team, JET EFDA Contributors, *Plasma Phys. Controll. Fusion* **2013**, *55*, 124039.

[36] P. J McCarthy, P. Martin, W. Schneider, The CLISTE interpretive equilibrium code, **1999**.

[37] L. Spitzer, R. Härm, *Phys. Rev.* **1953** March, *89*, 977.

[38] M. Hoelzl, S. Guenter, I. G. J. Classen, Q. Yu, the TEXTOR Team, E. Delabie, *Nucl. Fusion* **2009**, *49*, 115009.

[39] R. C. Malone, R. L. McCrory, R. L. Morse, *Phys. Rev. Lett.* **1975** March, *34*, 721.

[40] O. Sauter, C. Angioni, Y. R. Lin-Liu, *Phys. Plasmas* **1999**, *6*, 2834. https://doi.org/10.1063/1.873240.

[41] E. Viezzer, T. Puetterich, C. Angioni, A. Bergmann, R. Dux, E. Fable, R. M. McDermott, U. Stroth, E. Wolfrum, the ASDEX Upgrade Team, *Nucl. Fusion* **2014**, *54*, 012003.

[42] E. Wolfrum, A. Burckhart, R. Fischer, N. Hicks, C. Konz, B. Kurzan, B. Langer, T. PÃijtterich, H. Zohm, the ASDEX Upgrade Team, *Plasma Phys. Controll. Fusion* **2009**, *51*, 124057.

[43] A. Burckhart, E. Wolfrum, R. Fischer, K. Lackner, H. Zohm, the ASDEX Upgrade Team, *Plasma Phys. Controll. Fusion* **2010**, *52*, 105010.

[44] P. B. Snyder, T. H. Osborne, K. H. Burrell, R. J. Groebner, A. W. Leonard, R. Nazikian, D. M. Orlov, O. Schmitz, M. R. Wade, H. R. Wilson, *Phys. Plasmas* **2012**, *19*, 056115. https://doi.org/10.1063/1.3699623.

[45] A. Diallo, J. W. Hughes, M. Greenwald, B. LaBombard, E. Davis, S.-G. Baek, C. Theiler, P. Snyder, J. Canik, J. Walk, T. Golfinopoulos, J. Terry, M. Churchill, A. Hubbard, M. Porkolab, L. Delgado-Aparicio, M. L. Reinke, A. White, Alcator C-Mod team, *Phys. Rev. Lett.* **2014** March, *112*, 115001.

[46] F. M. Laggner, E. Wolfrum, M. Cavedon, F. Mink, E. Viezzer, M. G. Dunne, P. Manz, H. Doerk, G. Birkenmeier, R. Fischer, S. Fietz, M. Maraschek, M. Willensdorfer, F. Aumayr, the EUROfusion MST1 Team, the ASDEX Upgrade Team, *Plasma Phys. Controll. Fusion* **2016**, *58*, 065005.

[47] F. Mink, M. Hoelzl, E. Wolfrum, F. Orain, M. Dunne, A. Lessig, S. Pamela, P. Manz, M. Maraschek, G. T. A. Huijsmans, M. Becoulet, F. M. Laggner, M. Cavedon, K. Lackner, S. Günter, U. Stroth, the ASDEX Upgrade Team, *Nucl. Fusion* **2018**, *58*, 026011.

[48] C. P. Perez, H. R. Koslowski, G. T. A. Huysmans, T. C. Hender, P. Smeulders, B. Alper, E. de la Luna, R. J. Hastie, L. Meneses, M. F. F. Nave, V. Parail, M. Zerbini, J.-E. Contributors, *Nucl. Fusion* **2004**, *44*(5), 609.

[49] M. Bécoulet, M. Kim, G. Yun, S. Pamela, J. Morales, X. Garbet, G. T. A. Huijsmans, C. Passeron, O. Fevrier, M. Hoelzl, A. Lessig, F. Orain, *Nucl. Fusion* **2017**, *57*, 116059.

[50] F. Orain, M. Bécoulet, G. T. A. Huijsmans, G. Dif-Pradalier, M. Hoelzl, J. Morales, X. Garbet, E. Nardon, S. Pamela, C. Passeron, G. Latu, A. Fil, P. Cahyna, *Phys. Rev. Lett.* **2015** January, *114*, 035001.

[51] G. T. A. Huysmans, S. E. Sharapov, A. B. Mikhailovskii, W. Kerner, *Phys. Plasmas* **2001**, *8*, 4292. https://doi.org/10.1063/1.1398573.

[52] J. A. Morales, M. BÃlcoulet, X. Garbet, F. Orain, G. Dif-Pradalier, M. Hoelzl, S. Pamela, G. T. A. Huijsmans, P. Cahyna, A. Fil, E. Nardon, C. Passeron, G. Latu, *Phys. Plasmas* **2016**, *23*, 042513. https://doi.org/10.1063/1.4947201.

[53] I. Krebs, M. Hoelzl, K. Lackner, S. Guenter, *Phys. Plasmas* **2013**, *20*, 082506. https://doi.org/10.1063/1.4817953.

[54] R. P. Wenninger, H. Reimerdes, O. Sauter, H. Zohm, *Nucl. Fusion* **2013**, *53*, 113004.

[55] R. P. Wenninger, H. Zohm, J. E. Boom, A. Burckhart, M. G. Dunne, R. Dux, T. Eich, R. Fischer, C. Fuchs, M. Garcia-Munoz, V. Igochine, M. Hoelzl, L. N. C. Jr, T. Lunt, M. Maraschek, H. W. MÃijller, H. K. Park, P. A. Schneider, F. Sommer, W. Suttrop, E. Viezzer, the ASDEX Upgrade Team, *Nucl. Fusion* **2012**, *52*, 114025.

[56] B. Vanovac, E. Wolfrum, F. Mink, S. S. Denk, G. Harrer, P. Manz, F. M. Laggner, M. Cavedon, G. Birkenmeier, E. Viezzer, M. G. Dunne, M. Willensdorfer 2, M. Hoelzl, F. Orain, N. C. Luhmann Jr., the ASDEX Upgrade Team and the EUROfusion MST1 Team ECEI and magnetic measurements during inter-ELM modes 16th International Workshop in H-mode Physics and Transport Barriers, 2017, Saint-Petersburg

[57] F. Mink, E. Wolfrum, M. Maraschek, H. Zohm, L. Horvath, F. M. Laggner, P. Manz, E. Viezzer, U. Stroth, the ASDEX Upgrade Team, *Plasma Phys. Controll. Fusion* **2016**, *58*, 125013.

[58] F. Mink, personal communication, **2017**.

[59] M. Hoelzl, S. Günter, ASDEX Upgrade Team, in *38th European Physical Society Conference on Plasma Physics (EPS)*, Strasbourg, France, pp. P2.078.

[60] M. N. Rosenbluth, R. Z. Sagdeev, J. B. Taylor, G. M. Zaslavski, *Nucl. Fusion* **1966**, *6*(4), 297.

[61] E. Trier, E. Wolfrum, M. Willensdorfer, Q. Yu, F. Ryter, C. Angioni, F. Orain, M. Hoelzl, M. G. Dunne, S. Denk, J. C. Fuchs, R. Fischer, P. Hennequin, B. Kurzan, F. Mink, A. Mlynek, T. Odstrcil, P. A. Schneider, U. Stroth, B. Vanovac, the ASDEX Upgrade Team, the EUROfusion MST1 Team, *Plasma Phys. Controll. Fusion* (Submitted).

[62] R. S. MacKay, *Phys. D Nonlinear Phenomena* **1983**, *7*(1), 283.

[63] A. B. Rechester, T. H. Stix, *Phys. Rev. A* **1979** April, *19*, 1656.

[64] F. A. Volpe, J. Kessler, H. Ali, T. E. Evans, A. Punjabi, *Nucl. Fusion* **2012**, *52*, 054017.

[65] H. Wobig, *Zeitschrift für Naturforschung A* **1987**, *42*, 1054.

[66] T. Eich, A. Herrmann, J. Neuhauser, R. Dux, J. C. Fuchs, S. GÃijnter, L. D. Horton, A. Kallenbach, P. T. Lang, C. F. Maggi, M. Maraschek, V. Rohde, W. Schneider, the ASDEX Upgrade Team, *Plasma Phys. Controll. Fusion* **2005**, *47*(6), 815.

[67] T. Eich, A. Kallenbach, W. Fundamenski, A. Herrmann, V. Naulin, *J. Nucl. Mater.* **2009**, *390*(Supplement C), 760 Proc. 18th International Conference on Plasma-Surface Interactions in Controlled Fusion Device.

[68] F. Orain, M. Becoulet, J. Morales, G. T. A. Huijsmans, G. Dif-Pradalier, M. Hoelzl, X. Garbet, S. Pamela, E. Nardon, C. Passeron, G. Latu, A. Fil, P. Cahyna, *Plasma Phys. Controll. Fusion* **2015**, *57*, 014020.

[69] S. Pamela, T. Eich, L. Frassinetti, B. Sieglin, S. Saarelma, G. Huijsmans, M. Hoelzl, M. Becoulet, F. Orain, S. Devaux, I. Chapman, I. Lupelli, E. Solano, JET Contributors, *Plasma Phys. Controll. Fusion* **2016**, *58*, 014026.

[70] S. J. P. Pamela, G. T. A. Huijsmans, T. Eich, S. Saarelma, I. Lupelli, C. F. Maggi, C. Giroud, I. T. Chapman, S. F. Smith, L. Frassinetti, M. Becoulet, M. Hoelzl, F. Orain, S. Futatani, JET Contributors, *Nucl. Fusion* **2017**, *57*, 076006.

[71] T. Eich, B. Sieglin, A. J. Thornton, M. Faitsch, A. Kirk, A. Herrmann, W. Suttrop, *Nucl. Mater. Energy* **2017**, *12*, 84.

[72] M. Willensdorfer, T. B. Cote, C. C. Hegna, W. Suttrop, H. Zohm, M. Dunne, E. Strumberger, G. Birkenmeier, S. S. Denk, F. Mink, B. Vanovac, L. C. Luhmann, *Phys. Rev. Lett.* **2017** August, *119*, 085002.

[73] P. A. Schneider, E. Wolfrum, M. G. Dunne, R. Dux, A. Gude, B. Kurzan, T. Puetterich, S. K. Rathgeber, J. Vicente, A. Weller, R. Wenninger, the ASDEX Upgrade Team, *Plasma Phys. Controll. Fusion* **2014**, *56*, 025011.

[74] D.C. van Vugt, G.T.A. Huijsmans, M. Hoelzl, L.P.J. Kamp, N.J. Lopes Cardoso, A. Loarte, Kinetic simulations of W impurity transport by ELMs. 44th European Physical Society Conference on Plasma Physics (EPS), Belfast, Northern Ireland, P2.140 (06/2017).

[75] R. Dux, A. Janzer, T. Puetterich, ASDEX Upgrade Team, *Nucl. Fusion* **2011**, *51*, 053002.

[76] F. Liu, G. T. A. Huijsmans, A. Loarte, A. M. Garofalo, W. M. Solomon, M. Hoelzl, B. Nkonga, S. Pamela, M. Becoulet, F. Orain, D. Van Vugt, *Plamas Phys. Controll. Fusion* **2018**, *60*, 014039.

[77] F. Liu, G. T. A. Huijsmans, A. Loarte, A. M. Garofalo, W. M. Solomon, P. B. Snyder, M. Hoelzl, L. Zeng, *Nucl. Fusion* **2015**, *55*, 113002.

[78] P. T. Lang, A. W. Degeling, J. B. Lister, Y. R. Martin, P. J. M. Carthy, A. C. C. Sips, W. Suttrop, G. D. Conway, L. Fattorini, O. Gruber, L. D. Horton, A. Herrmann, M. E. Manso, M. Maraschek, V. Mertens, A. Mäijck, W. Schneider, C. Sihler, W. Treutterer, H. Zohm, ASDEX Upgrade Team, *Plasma Phys. Controll. Fusion* **2004**, *46*(11), L31.

[79] G. T. A. Huysmans, S. Pamela, E. van der Plas, P. Ramet, *Plasma Phys. Controll. Fusion* **2009**, *51*, 124012.

[80] P. T. Lang, K. Lackner, M. Maraschek, B. Alper, E. Belonohy, K. Gäal, J. Hobirk, A. Kallenbach, S. Kãalvin, G. Kocsis, C. P. P. von Thun, W. Suttrop, T. Szepesi, R. Wenninger, H. Zohm, the ASDEX Upgrade Team, JET-EFDA Contributors, *Nucl. Fusion* **2008**, *48*, 095007.

[81] H. R. Strauss, W. Park, *Phys. Plasmas* **1998**, *5*, 2676. https://doi.org/10.1063/1.872955.

[82] F. J. Artola, G. T. A. Huysmans, M Hoelzl, P Beyer, A Loarte, Y Gribov, *Nucl. Fusion*, (Submitted).

[83] W. Suttrop, A. Kirk, R. Nazikian, N. Leuthold, E. Strumberger, M. Willensdorfer, M. Cavedon, M. Dunne, R. Fischer, S. Fietz, J. C. Fuchs, Y. Q. Liu, R. M. McDermott, F. Orain, D. A. Ryan, E. Viezzer, The ASDEX Upgrade Team, The DIII-D Team and The Eurofusion MST Team Experimental studies of high-confinement mode plasma response to non-axisymmetric magnetic perturbations in ASDEX Upgrade. *Plasma Phys. Control. Fusion* **2017**, *59*, 014049 http://dx.doi.org/10.1088/0741-3335/59/1/014049

[84] E. Nardon, M. Bécoulet, G. Huysmans, O. Czarny, *Phys. Plasmas* **2007**, *14*, 092501. https://doi.org/10.1063/1.2759889.

[85] M. Bécoulet, F. Orain, G. T. A. Huijsmans, S. Pamela, P. Cahyna, M. Hoelzl, X. Garbet, E. Franck, E. Sonnendrücker, G. Dif-Pradalier, C. Passeron, G. Latu, J. Morales, E. Nardon, A. Fil, B. Nkonga, A. Ratnani, V. Grandgirard, *Phys. Rev. Lett.* **2014** September, *113*, 115001.

[86] F. Orain, M. Hoelzl, E. Viezzer, M. Dunne, M. Becoulet, P. Cahyna, G. T. A. Huijsmans, J. Morales, M. Willensdorfer, W. Suttrop, A. Kirk, S. Pamela, S. Guenter, K. Lackner, E. Strumberger, A. Lessig, the ASDEX Upgrade Team, the EUROfusion MST1 Team, *Nucl. Fusion* **2017**, *57*, 022013.

[87] F. Orain, M. Hoelzl, M. Becoulet, G. T. A. Huijsmans, S. Pamela, J. Artola, F. Liu, S. Futatani, D. van Vugt, D. Hu, E. Nardon, C. Sommariva, V. Bandaru, F. Mink, S. Guenter, A. Lessig, M. Dunne, E. Viezzer, W. Suttrop, M. Willensdorfer, E. Wolfrum, K. Lackner, B. Vanovac, M. Faitsch, N. Schwarz, ASDEX Upgrade Team Edge Localized Modes and their control techniques: comparisons between modeling and experiments. The 25th European Fusion Programme Workshop, Dubrovnik, Croatia (11/2017) Invited Talk.